Appendix C: Additional model details

Model Formulation

Existing work on hierarchical models for tree mortality in second growth systems typically adopts an annual compounding framework to account for uneven census intervals (Hurst et al. 2011, Peng et al. 2011, Thorpe and Daniels 2012, Luo and Chen 2013, but see Yang and Huang 2013). This formulation makes incorporating yearly variables difficult. One solution has been to use a single average value for the predictor for a given census interval, but tree mortality responses may track yearly variation in variables and thus mortality trends may not be detected if the representative variable cannot be modeled at the yearly level. Hierarchical state-space models (Metcalf et al. 2009, Clark et al. 2012, Csilléry et al. 2013) address these challenges by explicitly modeling the latent unmeasured survival status of the tree in each year; then a yearly climate variable as well as yearly stand development variables can be directly included.

A note on estimation: in order to ensure that the prior for mean survival b is flat on the probability scale, it must be specified in the following way in BUGS:

```
>         i.overall<-logit(li.overall)
>         li.overall~dunif(0, 1)
```

Where `i.overall` is b, and `li.overall` is the inverse logit ("expit") of b. See Buoro et al. (2012) for more details on ensuring flat priors on the probability scale. We adopt their method only for the intercept b and not for the β^ks because doing so resulted in very slow mixing and did not appreciably change parameter estimates.

See Figure C1 for a graphical representation of the model.

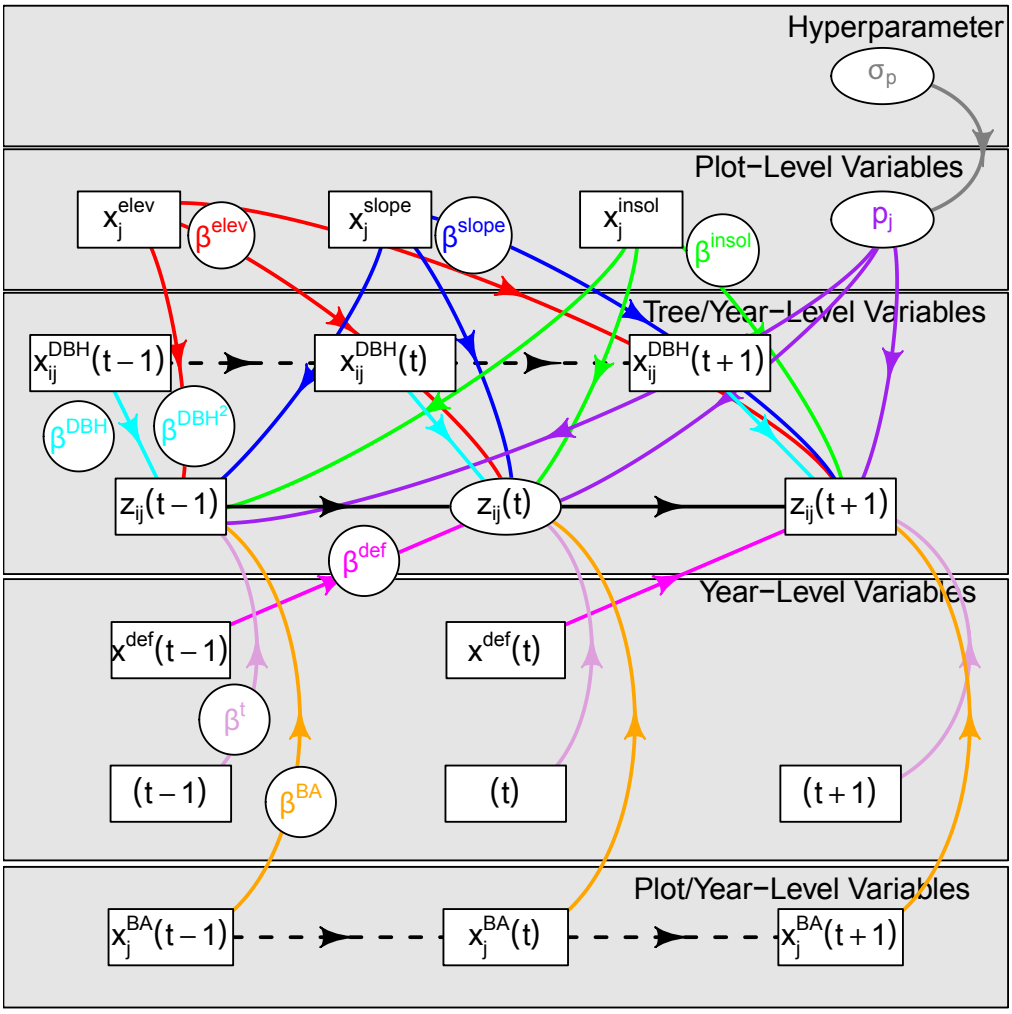

Figure C1: Diagram of the state-space model. Data are indicated in rectangles, with parameters and latent states to be estimated indicated in ellipses. Colored arrows indicate multiplication of data (rectangle) by a parameter (typically β, labeled circles) to be summed in the linear predictors for z. The black arrows indicate the process portion of the model wherein the current survival status is conditional on the previous survival status: if a tree is dead at time $(t-1)$, it remains dead at time t. This diagram is for tree i in plot j; imagine another such diagram for every tree in the inventory. Each linear predictor coefficient β is only labeled once, but every arrow of the same color also indicates that parameter. Note that we have depicted $z_{ij}(t-1)$ and $z_{ij}(t+1)$ as known states – observations – and $z_{ij}(t)$ as an unknown latent state to be estimated. Dashed black lines indicate variables which have been interpolated.

Prior sensitivity

The majority of model parameters were not sensitive to the priors chosen. We tested the final models with three alternative sets of priors: 1) for intercept, b, we tried a normal prior (precision = 1E-6) rather than uniform (0,1) for $expit(b)$; 2) for plot standard deviation, we tried a gamma(0.001, 0.001) on the precision scale (inverse gamma on the standard deviation scale); and 3) for the beta parameters for covariates, we tried a normal distribution with precision 1E-4, i.e. a standard deviation one order of magnitude smaller.

Beta parameters in particular showed little difference based on this smaller standard deviation (larger precision; see Fig. C2). Requiring the prior to be weakly informative on b rather than $expit(b)$ causes slight shifts for most species (biased towards higher survival), but a large shift for black oak and a moderate shift for tanoak (Fig. C3). We take this to mean that most species are weakly sensitive to the choice of prior, but that for species with very high survival and less data (i.e. black oak), the prior has a strong effect and ensuring that it is uninformative on the probability scale, as we have done in the main paper, is very important.

The plot standard deviation posterior did show some sensitivity (Fig. C4). In particular, by using an inverse gamma prior, we see that for two species with small plot standard deviations (Douglas-fir and sugar pine), weighting values closer to zero more highly does reduce the parameter estimates and slows mixing. On the other hand, for two species (white fir and black oak), the inverse gamma prior prevents the MCMC from getting 'stuck' at zero because it has zero weight at zero. This causes the posterior to align completely with the non-zero mode demonstrated for these species in Appendix F. For all other species, changing the plot standard deviation prior makes no appreciable difference in the resulting posterior. We interpret these results to indicate that the prior chosen in the main text (which is flat on the standard deviation scale) is a reasonable choice, in contrast to the effectively uninformative normal prior on the precision scale which results in an inverse gamma prior on the standard deviation scale. We additionally note that the standard deviations for white fir and black oak are likely to be significant and the secondary node at zero seen in Appendix F is an artifact of the MCMC sampler.

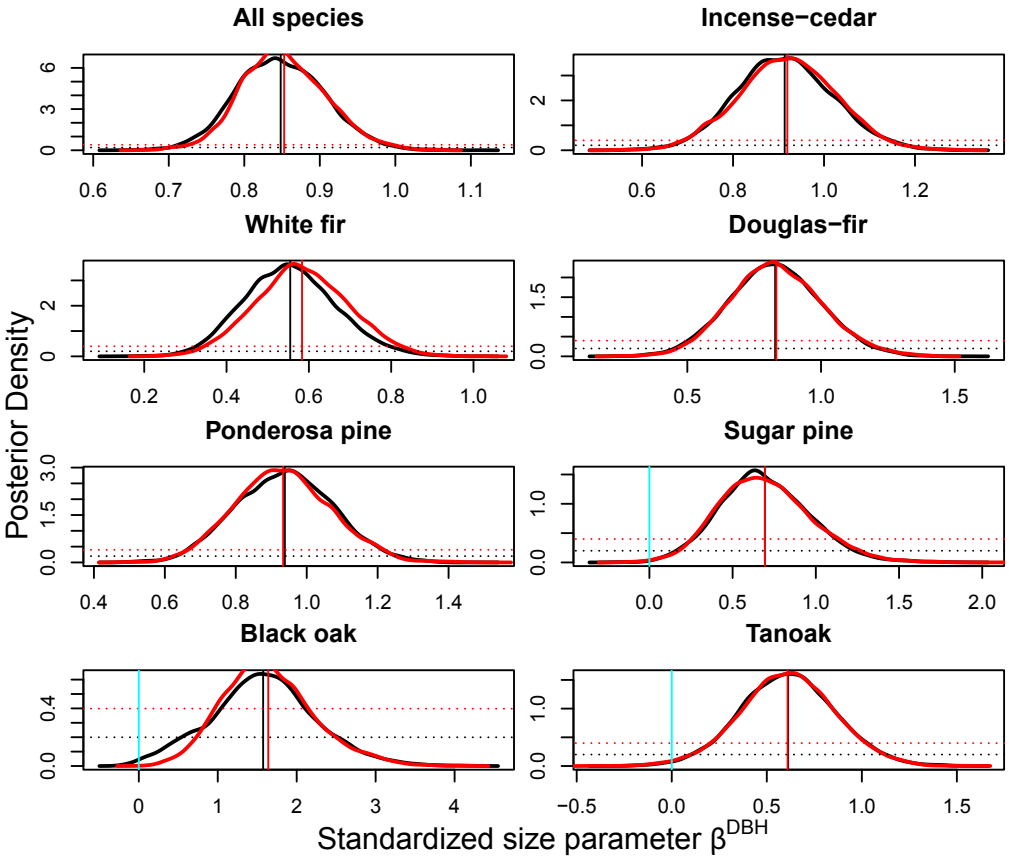

Figure C2: Sensitivity of posteriors for linear size, β^{DBH}, to different normal priors, one with precision 1E-6 (black, final model), and one with precision 1E-4 (red). Solid lines are posteriors; dotted lines are priors, multiplied by various factors of 10 to make their shape visible against the posteriors. Vertical solid lines are posterior means, and (where visible), cyan vertical lines indicate initial values for the MCMC chain.

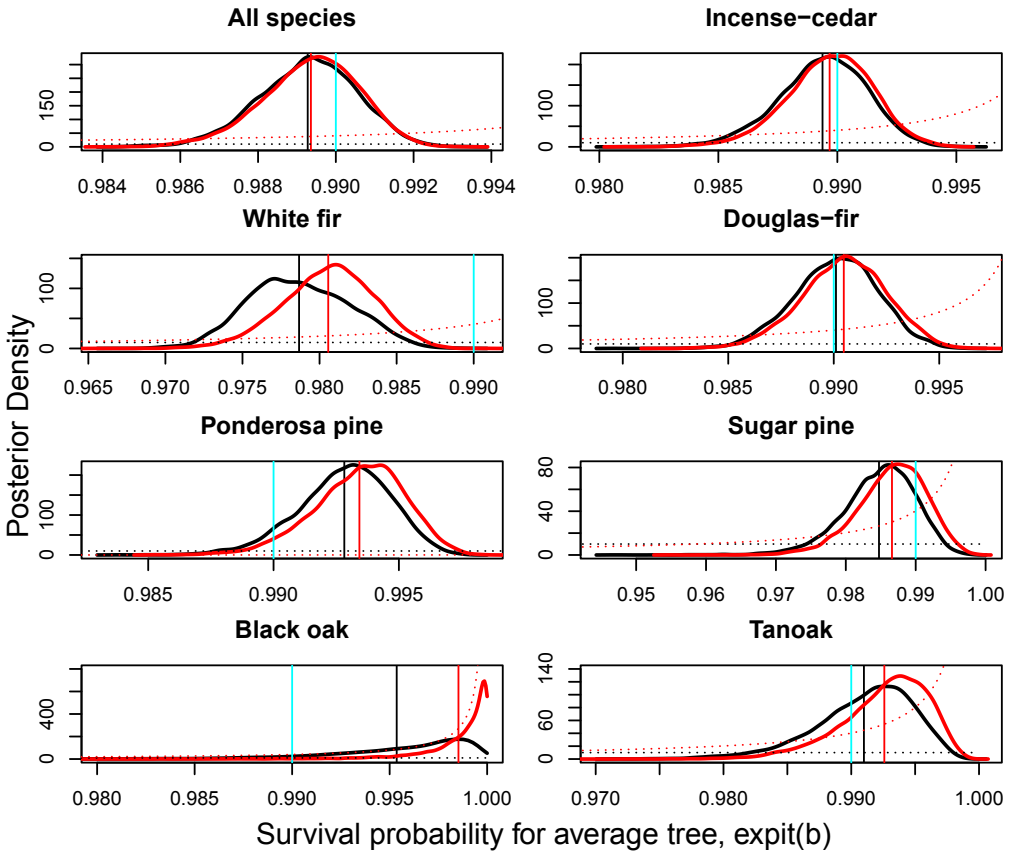

Figure C3: Sensitivity of posteriors for the survival of an average tree, $expit(b)$, to different priors, one uniform on $expit(b)$ (black, final model), and one normal (precision 1E-6) on b (red). Solid lines are posteriors; dotted lines are priors, multiplied by various factors of 10 to make their shape visible against the posteriors. Vertical solid lines are posterior means, and (where visible), cyan vertical lines indicate initial values for the MCMC chain.

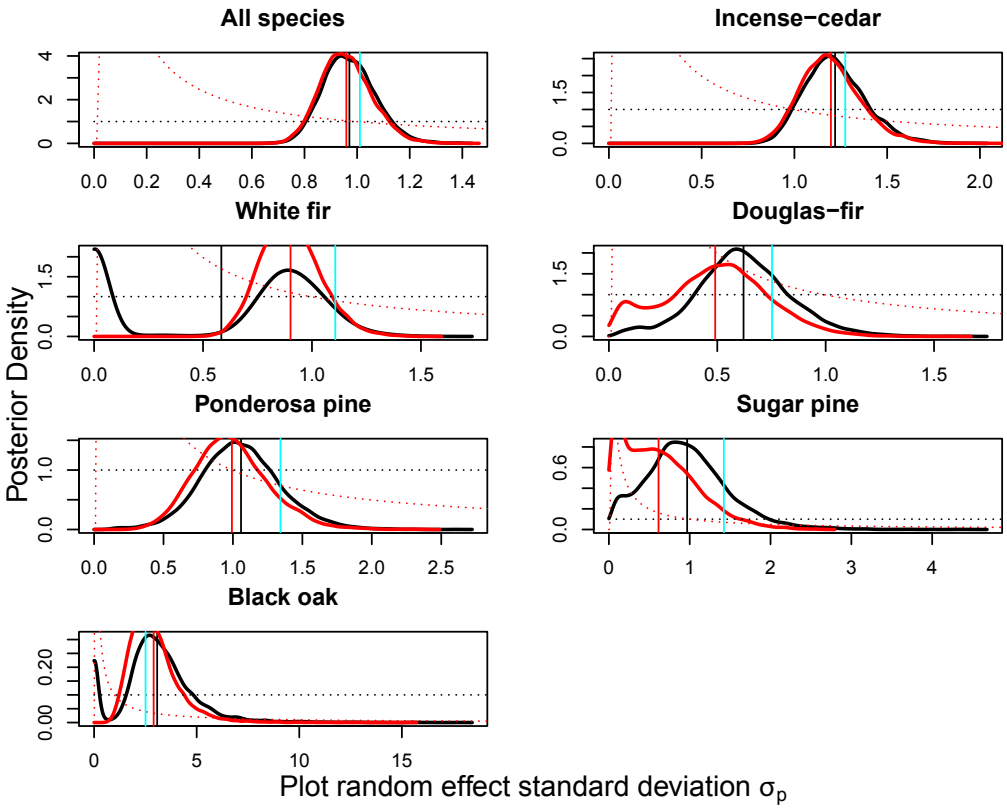

Figure C4: Sensitivity of posteriors for the plot random effect standard deviation, σ_p, to different priors, one uniform on the standard deviation from zero to 100 (black, final model), and one gamma (0.001, 0.001) on the precision (inverse-gamma on the standard deviation, red). Solid lines are posteriors; dotted lines are priors, multiplied by various factors of 10 to make their shape visible against the posteriors. Vertical solid lines are posterior means, and (where visible), cyan vertical lines indicate initial values for the MCMC chain.

Standardizing explanatory variables

We have standardized the original variables by centering (subtracting the mean of the explanatory variable μ_{x^k}) and scaling (dividing by the standard deviation of the explanatory variable σ_{x^k}):

$$x^k(t)' = \frac{x^k(t) - \mu_{x^k}}{\sigma_{x^k}} \tag{C.1}$$

The model we have estimated is in terms of these standardized variables:

$$logit(\phi_{ij}(t)') = {\beta_{0_j}}' + \sum_k \beta^{k\prime} x_{ij}^k(t)' \tag{C.2}$$

Rewriting this in terms of the original variables:

$$logit(\phi_{ij}(t)') = {\beta_{0_j}}' + \sum_k \beta^{k\prime} \frac{x^k(t) - \mu_{x^k}}{\sigma_{x^k}} \tag{C.3}$$

We want to keep the variables centered but return them to the scale of the original variables, so we want to write this equation in terms of a centered variable:

$$x^k(t)'' = x^k(t) - \mu_{x^k} \tag{C.4}$$

Rewriting the model equation with respect to the double-primed variables:

$$logit(\phi_{ij}(t)'') = {\beta_{0_j}}'' + \sum_k \beta^{k\prime\prime} \frac{x^k(t)''}{\sigma_{x^k}} \tag{C.5}$$

We can see that the intercept ${\beta_{0_j}}'' = {\beta_{0_j}}' = \beta_{0_j}$ (and b and p_j along with it); but that the coefficient for $x^k(t)$ must be divided by σ_{x^k}:

$$\beta^{k\prime\prime} = \beta^{k\prime} / \sigma_{x^k} \tag{C.6}$$

The quadratic term for size, (β^{DBH^2}), would need to be divided by $\sigma^2_{x^{DBH}}$.

References

Buoro, M., E. Prévost, and O. Gimenez. 2012. Digging through model complexity: using hierarchical models to uncover evolutionary processes in the wild. Journal of evolutionary biology **25**:2077–90.

Clark, J. S., D. M. Bell, M. Kwit, A. Stine, B. Vierra, and K. Zhu. 2012. Individual-scale inference to anticipate climate-change vulnerability of biodiversity. Philosophical Transactions of the Royal Society of London. Series B, Biological Sciences **367**:236–46.

Csilléry, K., M. Seignobosc, V. Lafond, G. Kunstler, and B. Courbaud. 2013. Estimating long-term tree mortality rate time series by combining data from periodic inventories and harvest reports in a Bayesian state-space model. Forest Ecology and Management **292**:64–74.

Hurst, J. M., R. B. Allen, D. A. Coomes, and R. P. Duncan. 2011. Size-specific tree mortality varies with neighbourhood crowding and disturbance in a Montane Nothofagus forest. PloS one **6**:e26670.

Luo, Y., and H. Y. H. Chen. 2013. Observations from old forests underestimate climate change effects on tree mortality. Nature Communications **4**:1655.

Metcalf, C. J. E., S. M. McMahon, and J. S. Clark. 2009. Overcoming data sparseness and parametric constraints in modeling of tree mortality: a new nonparametric Bayesian model. Canadian Journal of Forest Research **39**:1677–1687.

Peng, C., Z. Ma, X. Lei, Q. Zhu, H. Chen, W. Wang, S. Liu, W. Li, X. Fang, and X. Zhou. 2011. A drought-induced pervasive increase in tree mortality across Canada's boreal forests. Nature Climate Change **1**:467–471.

Thorpe, H. C., and L. D. Daniels. 2012. Long-term trends in tree mortality rates in the Alberta foothills are driven by stand development. Canadian Journal of Forest Research **42**:1687–1696.

Yang, Y., and S. Huang. 2013. A Generalized Mixed Logistic Model for Predicting Individual Tree Survival Probability with Unequal Measurement Intervals. Forest Science **59**:177–187.